The Relative Potential Field as a Novel Physics-Inspired Method for Image Analysis

X. D. ZHUANG[1] and N. E. MASTORAKIS[1,2]
1. WSEAS Headquarters
Agiou Ioannou Theologou 17-23, 15773, Zografou, Athens, GREECE
xzhuang@worldses.org, xzh_wseas@tom.com
2. Department of Computer Science, Military Institutions of University Education,
Hellenic Naval Academy, Terma Hatzikyriakou, 18539, Piraeus, GREECE
mastor@wseas.org http://www.wseas.org/mastorakis

Abstract: - In this paper, the relative potential field is proposed as a novel image transform inspired by the physical electro-static field. A general form of image potential field is presented, based on which the relative potential is defined by introducing the factor of gray-scale difference into the potential field. The properties of the relative potential are investigated experimentally and analyzed, based on which an image segmentation method is proposed by region division and merging in the relative potential field. Experimental results prove the effectiveness of the proposed image segmentation method, and also indicate the promising application of the relative potential in image processing tasks.

Key-Words: - Relative potential field, electro-static, image transform, image segmentation

1 Introduction

Image transform is an important way for feature extraction and analysis [1-7]. Most currently applied transforms change the signal form between the time or space domain and the parameter domain, such as the mathematically reversible transforms including Fourier transform (transform between the time or space domain and the frequency domain) and the Wavelet transform (transform between the time or space domain and the time-scale or space-scale domain) [8-12]. Novel image transform has become an important branch of the development of image processing techniques [3-7].

In recent years, physics-inspired methodology has attracted more and more research interest, which exhibits promising ability of effective feature extraction and analysis [13-22]. The fundamental principle underlying the physical field inspired methods is the transform from one form of the field to another (i.e. from field source to its potential) so that the feature of interest can be revealed [13,14,21,22].

In this paper, a novel image transform named the relative potential field is proposed based on an electro-static analogy. The relationship between the potential field and the source in physics is exploited to define the novel image transform for image structure representation and analysis. Image segmentation is implemented by region division and merging in the relative potential field.

2 The relative potential field of digital images

In physics, the electro-static potential field is determined by the source (i.e. the charge distribution) [23-26]. Therefore, the potential field can reflect some characteristics of the source. This relationship between the field and its source can be exploited in image transform, in which the image is regarded as the source (i.e. the pixels are regarded as discrete charges) and the generated virtual field may reveal important features of the image. The attraction of physical field inspired methods is the possibility of a natural representation of image structure or components without artificially set parameters such as the thresholds in image segmentation. In this paper, a general form of virtual potential field for digital images is proposed, which is inspired by the physical electro-static field.

The formula of the physical electro-static potential generated by a charge q is as following [23-26]:

$$V = \frac{1}{4\pi\varepsilon} \cdot \frac{q}{r} \tag{1}$$

where V is the electro-static potential at a space point. q is the charge quantity. r is the distance between the charge and the space point. ε is a physical constant.

For a charge distribution ρ in the space, the potential generated by ρ on the point (x,y) is as following [23-26]:

$$V = \frac{1}{4\pi\varepsilon}\int_V \frac{\rho \cdot d\tau}{r} \qquad (2)$$

where V is the electro-static potential at a space point. The integral in Equation (2) is for the whole region where the charge distribution ρ exists.

Many image processing techniques involves local operations in the image, i.e. local image features are extracted and analyzed [27-29]. Local image features usually have the form of a binary function $f(x,y)$ defined on the two-dimensional image plane. On the other hand, the analysis of the image also requires consideration of the neighbouring area of each image point in order to get practically useful results. For example, in some self-adaptive segmentation methods, local features are extracted and then the segmentation threshold for each point is determined adaptively according to its neighbouring area. It is indicated that the local and global analysis are both needed in image processing [30-36].

Generally speaking, neighbouring points have stronger relevance than remote points, i.e. the closer the distance, the stronger the relevance. In many image processing tasks, it is necessary to consider the balance between the strong local relevance of close neighbouring points and a wide range of weaker relevance of remote points. And a mathematical model is needed for the representation of the above local-global relevance between image points.

Equation (2) indicates that the potential of a charge q on a space point (i.e. the impact of q on that point) is in direct proportion to the reciprocal of the distance r. The mathematical form of the distance reciprocal in Equation (2) inspires the representation of the local-global relevance between image points. For a point p in the space, the near charge distribution in the small local neighboring area has greater impact on p's potential than remote charge distribution. On the other hand, no matter how far the distance is, remote charge distribution still has relatively weak impact on p's potential. Moreover, the accumulation of the weak impacts of wide-range remote charge distribution can not be neglected. The above characteristic of the distance reciprocal form in Equation (2) is quite suitable for the requirement of image analysis that both local and global relevance between image points should be considered.

The electro-static potential has a suitable mathematical form to model the local-global relevance of image points. A general form of virtual image potential field is proposed with the electro-static analogy. For image analysis, not only the distance between two image points but also the relationship between their gray-scale or color should be considered. Therefore, a general continuous form of image virtual potential field is proposed as:

$$V_c^k(x,y) = A \cdot \int_a\int_b \frac{f(g(a,b), g(x,y))}{r^k_{(a,b)\to(x,y)}} da \cdot db \qquad (3)$$

where $V_c^k(x,y)$ is the continuous image potential value on point (x,y). A is a predefined constant value. g is the gray-scale value of image points. f is a function that defined according to specific image processing tasks representing the relationship between the gray-scale values of point (x,y) and (a,b). r is the distance between (x,y) and (a,b). k is a constant that affect the reciprocal's decreasing rate with the increasing distance r. The double integral in Equation (3) is on the two-dimensional image plane. For a specific processing task, the function f and the constants A, k should be pre-defined according to the specific processing purpose.

For digital images, the general discrete form of image virtual potential field is proposed as the discrete form of Equation (4):

$$V_d^k(x,y) = A \cdot \sum_{\substack{j=0 \\ (j\neq x \text{ or } i\neq y)}}^{ROW-1} \sum_{i=0}^{COL-1} \frac{f(g(i,j), g(x,y))}{r^k_{(i,j)\to(x,y)}} \qquad (4)$$

where $V_d^k(x,y)$ is the discrete image potential on point (x,y). A is a predefined constant value. ROW and COL are the height and width of the digital image respectively. g is the gray-scale value of image points. f is a function that defined according to specific image processing tasks representing the relationship between the gray-scale values of point (x,y) and (i,j). r is the distance between (x,y) and (i,j). k is a constant that affect the reciprocal's decreasing rate with the increasing distance r.

For some important image processing tasks such as segmentation and edge detection, the difference between pixel gray-scale values are the factor of major consideration. In this paper the relative potential is proposed for gray-scale images based on the general form of discrete image potential, where the function $f(g(i,j), g(x,y))$ is specialized as the difference between the gray-scale values of the two image points (x,y) and (i,j):

$$V_R^k(x,y) = A \cdot \sum_{\substack{j=0 \\ (j\neq x \text{ or } i\neq y)}}^{ROW-1} \sum_{i=0}^{COL-1} \frac{g(i,j) - g(x,y)}{r^k_{(i,j)\to(x,y)}} \qquad (5)$$

where $V_R^k(x,y)$ is the relative potential of the digital image on point (x,y). A is a predefined constant value. ROW and COL are the height and width of the digital image respectively. g is the gray-scale value of image points. r is the distance between (x,y)

and (i,j). k is a constant that affect the reciprocal's decreasing rate with the increasing distance r.

Compared with the mathematic form of the electro-static potential, the proposed relative potential has two major differences. One is the replacement of the discrete charge with the gray-scale difference, which can make the relative potential represents the difference of one image point between others. The other is the k-th power of the distance r. Thus the adjustment of the value k can change the decreasing rate of the relevance between image points with the increasing distance r according to the requirement of a specific task.

3 The property of the relative potential field

In Equation (5), the relevance between two image points with distance r is represented quantitatively by the reciprocal of r^k. The value of relative potential is virtually the weighted sum of the gray-scale difference between the image point on (x,y) and all other points, and the weight is the factor of relevance, i.e. the reciprocal of r^k. To investigate the properties of the relative potential field, experiments are carried out for a series of simple test images with the size of 128×128. When computing the relative potential values, the constant k in Equation (5) is pre-defined as k=1. Fig. 1 To Fig. 3 are the results for some typical test images.

Fig. 1(a) to Fig. 3(a) are the original test images. Fig. 1(b) to Fig. 3(b) are the relative potential value distributions of the corresponding test images, where larger gray-scale represents larger relative potential. Fig. 1(c) to Fig. 3(c) record the sign of each relative potential value, where white points have positive values and black points have negative values. The results shown in Fig. 1(c) to Fig. 3(c) indicate that the sign of the relative potential values will reverse across the boundary of two adjacent regions, which may be exploited in the division of different regions in the image.

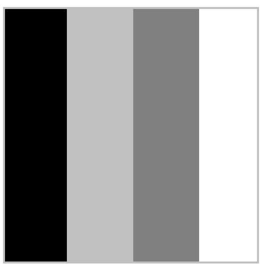

(a) The image Test1

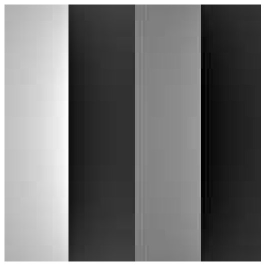

(b) The relative potential value distributions

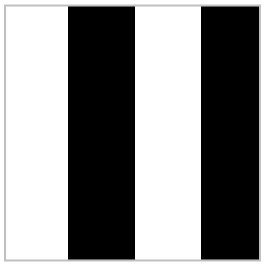

(c) The sign of each relative potential value

Fig. 1 The relative potential field of image Test1

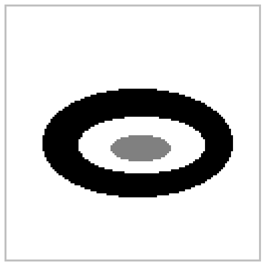

(a) The image Test2

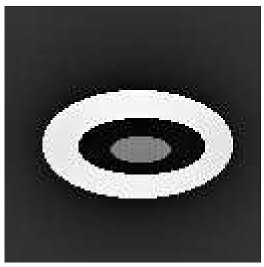

(b) The relative potential value distributions

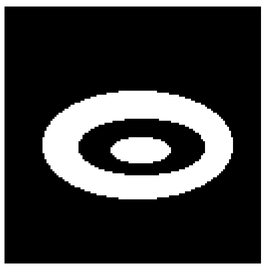

(c) The sign of each relative potential value

Fig. 2 The relative potential field of image Test2

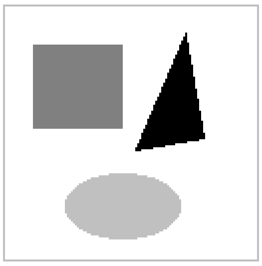

(a) The image Test3

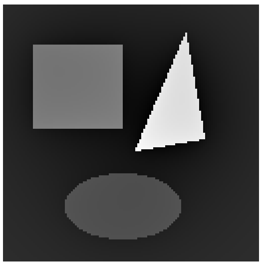

(b) The relative potential value distributions

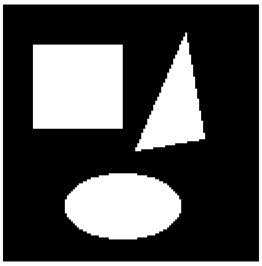

(c) The sign of the relative potential value

Fig. 3 The relative potential field of image Test3

According to the definition of the image relative potential in Equation (5), the relative potential value of a point p is mainly affected by its local neighboring area. The local neighboring area consists of two classes of points. One class is those in the same region of p (i.e. with similar gray-scale of p), the other is those in the different region. For simple test images, the gray-scale difference in the same region is zero. Thus the relative potential of p is mainly affected by the gray-scale difference between p's region and its adjacent region. Suppose A and B are two adjacent regions shown in Fig. 4. p_a and p_b are two border points at different border sides. p_a is in region A and p_b is in region B. g_a and g_b are the gray-scale of region A and B respectively. According to the above discussion, the sign of p_a 's relative potential is determined by g_b - g_a, while the sign of p_b 's relative potential is determined by g_a - g_b. Thus the signs of p_a and p_b are opposite. This is why the sign of the relative potential will reverse across the region border. This property of the relative potential field can be exploited in image analysis.

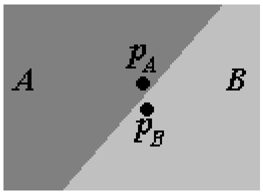

Fig. 4 p_a and p_b on different sides of the region border

On the other hand, the experimental results of some other test images indicate that the sign reverse of relative potential is not only across region borders but also possible within a region. Fig. 5 shows such a case, where the sign reverse occurs in the middle region of the three in the image. This is because within a region the near points in the neighbouring area have the same gray-scale, and the accumulation of weak affects from wide range of remote image points will have effect on the relative potential value. Thus sign reverse may occur within some region. Therefore, it can be concluded from the experimental results that the sign of relative potential will reverse across the region borders, and there is also possible sign reverse within a region.

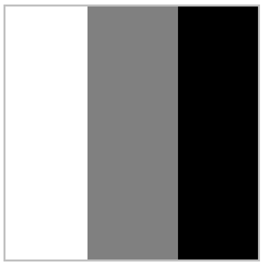

(a) The image Test4

(b) The relative potential value distributions

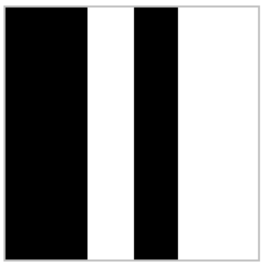

(c) The sign of each the relative potential value for Test4

Fig. 5 The relative potential of image Test4

4 Image segmentation based on the relative potential field

In the experimental results of the test images, it is shown that the sign of relative potential values are opposite in the two different adjacent regions. This can provide the basis of region division in images. In this paper, a method of image region division in the relative potential field is proposed as following:

***Step*1**: Calculate the relative potential field;

***Step*2**: Obtain the sign distribution of the relative potential field;

***Step*3**: Group the adjacent points with the same sign of relative potential into connected regions.

The obtained set of connected regions is the result of region division for the gray-scale image.

Fig. 6 to Fig. 8 are the region division results according to Fig.1 (c) to Fig. 3(c), where different regions are represented by different gray-scale values. The results indicate that the region division method is effective for simple test images.

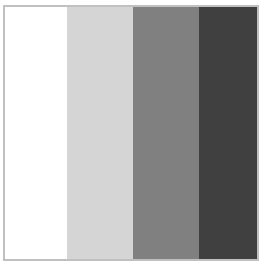

Fig. 6 The region segmentation result according to Fig.1 (c)

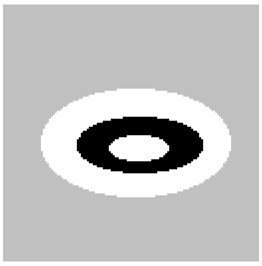

Fig. 7 The region segmentation result according to Fig.2 (c)

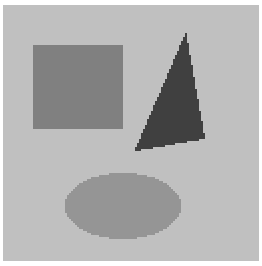

Fig. 8 The region segmentation result according to Fig.3 (c)

Real world images consist of much more complex region components than the simple test images. To investigate the effect of the above region division method on real world images, experiments are carried out for a series of typical real world images. The experimental results are shown from Fig. 9 to Fig. 12

(a) The broadcaster image

(b) The visualization of the relative potential field with k=1

(c) The visualization of the relative potential field with k=2

(d) The visualization of the relative potential field with k=3

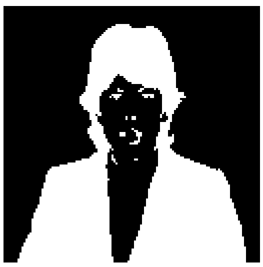

(e) The sign distribution of the relative potential in (b)

(f) The sign distribution of the relative potential in (c)

(g) The sign distribution of the relative potential in (d)

(h) The region division result for (e)

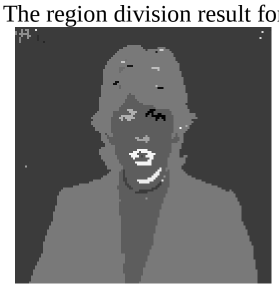

(i) The region division result for (f)

(j) The region division result for (g)

Fig. 9 The relative potential field and region division results for the broadcaster image

(a) The house image

(b) The visualization of the relative potential field with k=1

(c) The visualization of the relative potential field with k=2

(d) The visualization of the relative potential field with k=3

(e) The sign distribution of the relative potential in (b)

(f) The sign distribution of the relative potential in (c)


(g) The sign distribution of the relative potential in (d)


(h) The region division result for (e)


(i) The region division result for (f)


(j) The region division result for (g)

Fig. 10 The relative potential field and region division results for the house image

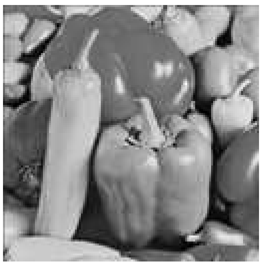
(a) The peppers image


(b) The visualization of the relative potential field with k=1


(c) The visualization of the relative potential field with k=2


(d) The visualization of the relative potential field with k=3


(e) The sign distribution of the relative potential in (b)


(f) The sign distribution of the relative potential in (c)


(g) The sign distribution of the relative potential in (d)

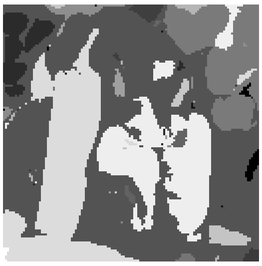
(h) The region division result for (e)


(i) The region division result for (f)

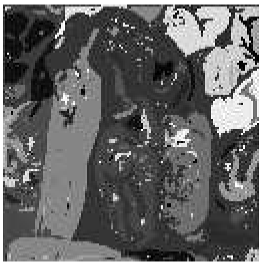
(j) The region division result for (g)

Fig. 11 The relative potential field and region division results for the peppers image


(a) The cameraman image


(b) The visualization of the relative potential field with k=1


(c) The visualization of the relative potential field with k=2


(d) The visualization of the relative potential field with k=3


(e) The sign distribution of the relative potential in (b)


(f) The sign distribution of the relative potential in (c)

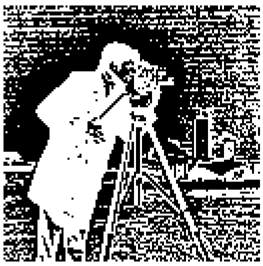
(g) The sign distribution of the relative potential in (d)


(h) The region division result for (e)

(i) The region division result for (f)

(j) The region division result for (g)

Fig. 12 The relative potential field and region division results for the cameraman image

Fig. 9(a) to Fig. 12(a) are the original images of the broadcaster, house, peppers and cameraman respectively. In the experiments, to investigate the influence of constant k (i.e. the relevance decreasing rate with increasing distance r) on image region division, relative potential field is calculated with k=1, 2 and 3 respectively. In the experiments, the results of relative potential field are visualized as gray-scale images. Fig. 9(b) to Fig. 12(b) are the results of relative potential field visualization with k=1 in Equation (5), where larger gray-scale values correspond to larger relative potential values. Fig. 9 (c) to Fig. 12(c) are the results of relative potential field visualization with k=2 in Equation (5). Fig. 9(d) to Fig. 12(d) are the results of relative potential field visualization with k=3 in Equation (5).

To investigate the sign distribution of the relative potential field, the sign of relative potential on each point is recorded in the experiment. Fig. 9(e) to Fig. 12(e) are the sign distribution of the relative potential in Fig. 9(b) to Fig. 12(b) respectively, where white points represent positive values and black points represent negative values. Fig. 9(f) to Fig. 12(f) are the sign distribution of the relative potential in Fig. 9(c) to Fig. 12(c) respectively. Fig. 9(g) to Fig. 12(g) are the sign distribution of the relative potential in Fig. 9(d) to Fig. 12(d) respectively.

The region division is carried out based on the sign distribution of the relative potential field. Fig. 9(h) to Fig. 12(h) show the region division results for Fig. 9(e) to Fig. 12(e) respectively, where different regions are represented by different gray-scale values. Fig. 9(i) to Fig. 12(i) show the region division results for Fig. 9(f) to Fig. 12(f) respectively. Fig. 9(j) to Fig. 12(j) show the region division results for Fig. 9(g) to Fig. 12(g) respectively. The region division results show that for real world images the region division method may obtain large amount of region elements in the image.

Table 1 shows the region numbers obtained by the region division method for the real world images with the constant k=1, 2, and 3 respectively. Table 1 indicates that larger value of k can obtain more detailed region division result, because larger value of k causes faster decreasing rate of the relevance between image points with the increasing distance r.

Table 1 The number of regions obtained with different k

	The number of regions obtained by the region division based on the sign distribution of the relative potential field		
	***k*=1**	***k*=2**	***k*=3**
broadcaster image	19	39	659
house image	85	268	946
peppers image	72	122	371
cameraman image	161	298	795

The region division results of real world images consist large amount of region elements due to the complexity of real world images. To obtain practically useful segmentation result, a region merging method is proposed for the region division results of real world images based on the gray-scale similarity of adjacent regions. First, an expected number of remaining regions after merging is given (usually by trail). Then the following steps are carried out to merge regions until the expected region number is reached:

***Step*1**: For each region in the image, calculate its average gray-scale value.

***Step*2**: Find the pair of neighboring regions with the least difference of the average gray-scale, and merge them into one region.

***Step*3**: If current region number is larger than the expected region number, return to ***Step*1**; otherwise, end the merging process.

The region merging results for the real world images are shown in Fig. 13 to Fig. 16, where different regions are represented by different gray-scale. Fig. 13(a) to Fig. 16(a) show the merging results of Fig. 9(h) to Fig. 12(h) respectively. Fig.

13(b) to Fig. 16(b) show the merging results of Fig. 9(i) to Fig. 12(i) respectively. Fig. 13(c) to Fig. 16(c) show the merging results of Fig. 9(j) to Fig. 12(j) respectively. The merging results indicate that larger value of *k* makes more detailed region division, and correspondingly the merging results can be more accurate.

(a) The merging result of Fig. 9(h)

(b) The merging result of Fig. 9(i)

(c) The merging result of Fig. 9(j)

Fig .13 The region merging results for the broadcaster image

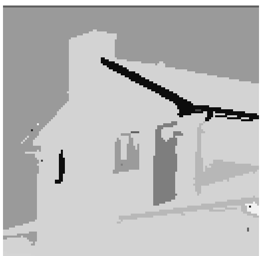

(a) The merging result of Fig. 10(h)

(b) The merging result of Fig. 10(i)

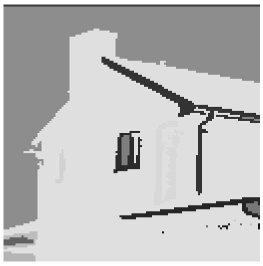

(c) The merging result of Fig. 10(j)

Fig. 14 The region merging results for the house image

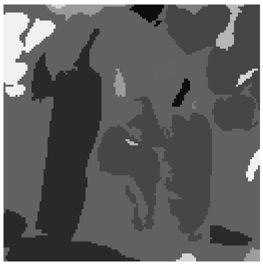

(a) The merging result of Fig. 11(h)

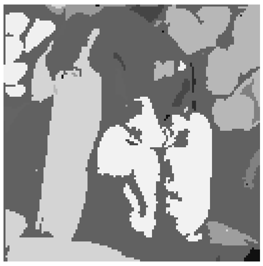

(b) The merging result of Fig. 11(i)

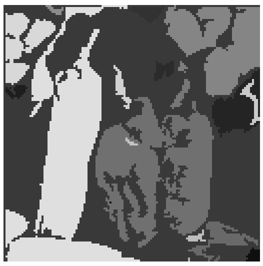

(c) The merging result of Fig. 11(j)

Fig. 15 The region merging results for the peppers image

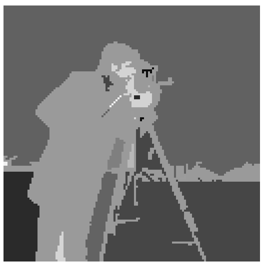

(a) The merging result of Fig. 12(h)

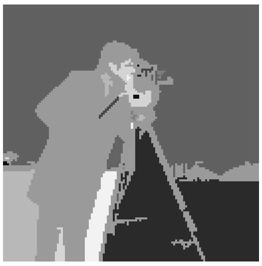

(b) The merging result of Fig. 12(i)

(c) The merging result of Fig. 12(j)

Fig. 16 The region merging results for the cameraman image

Based on the above discussions, in this paper a novel image segmentation method is proposed based on the relative potential field. The procedure of the segmentation is as following:

***Step*1**: Calculate the relative potential field;

***Step*2**: Carry out the region division based on the sign distribution of the relative potential field;

***Step*3**: Merge the region division result to a pre-defined number of regions.

The experimental results have proved the effectiveness of the proposed segmentation method.

5 Conclusion

The mathematical form of the physical electro-static potential provides a suitable model for the representation of the local-global relevance between image points. In this paper, the relative potential field is proposed with the electro-static analogy. The image structure information can be revealed by the field transform of relative potential. The experimental results indicate that the sign distribution of the relative potential field can serve as the basis for image region division, based on which an image segmentation method is proposed. Experimental results also prove the effectiveness of the proposed segmentation method. Further work will investigate the application of the relative potential field in other image processing tasks.

References:

[1] R.F. Edgar, Generation and application of image transforms, *Optics Technology*, Vol. 1, Issue 4, 1969, pp. 183-190.

[2] YuJin Zhang. *Image Engineering: Image Processing* (*2nd Edition*), TUP Press, Beijing, China, 2006.

[3] Wang Min, Zhang Yanning, Sun Jinqiu, Li Ying, Ma Miao, A Method of Image Transform Based on Linear Elements, *Fifth International Conference on Image and Graphics*, 2009, 2009, pp. 124-128.

[4] R. Memisevic, G. Hinton, Unsupervised Learning of Image Transformations, *Proceedings of IEEE Conference on Computer Vision and Pattern Recognition*, 2007, pp. 1-8.

[5] Lennart Wietzke, Oliver Fleischmann, Gerald Sommer, 2D Image Analysis by Generalized Hilbert Transforms in Conformal Space, *Proceedings of the 10th European Conference on Computer Vision: Part II*, 2008, pp. 638-649.

[6] Shou-Cheng Hsiung, J. H. Jeng, Image retrieval based on fractal transformation, *WSEAS Transactions on Information Science and Applications*, Vol. 2, No. 7, 2005, pp. 827-834.

[7] T. Kowaliw, W. Banzhaf, N. Kharma, S. Harding, Evolving novel image features using genetic programming-based image transforms, *Proceedings of the IEEE Congress on Evolutionary Computation*, 2009, pp. 2502-2507.

[8] Claude Gasquet, Patrick Witomski, *Fourier analysis and applications: filtering, numerical computation, wavelets*, Springer, 1999.

[9] Lokenath Debnath, *Wavelet transforms and their applications*, Springer, 2002.

[10] S. Mallat, A theory for multi-resolution signal decomposition: The wavelet representation, *IEEE Pat. Anal. Mach. Intell.*, Vol. 11, No. 7, 1989, pp. 674-693.

[11] R.N. Bracewell, *The Fourier Transform and Its Applications* (*Series in Electrical Engineering*), McGraw-Hill Book Company, New York, 1986.

[12] Jaime Gomez, Carmen Morato, Teresa Castellanos, Juan Seijas, Two different approaches to classification applying appropriate wavelets, *WSEAS Transactions on Systems*, Vol. 4, No. 12, 2005, pp. 2369-2375.

[13] D. J. Hurley, M. S. Nixon and J. N. Carter, Force field feature extraction for ear biometrics, *Computer Vision and Image Understanding*, Vol. 98, No. 3, 2005, pp. 491-512.

[14] X. D. Zhuang and N. E. Mastorakis, The Curling Vector Field Transform of Gray-Scale Images: A Magneto-Static Inspired Approach, *WSEAS Transactions on Computers*, Issue 3, Vol. 7, 2008, pp. 147-153.

[15] G. Abdel-Hamid and Y. H. Yang, Multiscale Skeletonization: An electrostatic field-based approach, *Proc. IEEE Int. Conference on Image Processing*, Vol. 1, 1994, pp. 949-953.
[16] Luo, B., Cross, A. D. and Hancock, E. R., Corner Detection Via Topographic Analysis of Vector Potential, *Pattern Recognition Letters*, Vol. 20, No. 6, 1999, pp. 635-650.
[17] Andrew D. J. Cross and Edwin R. Hancock, Scale-space vector field for feature analysis, *Proceedings of the IEEE Computer Society Conference on Computer Vision and Pattern Recognition*, 1997, pp. 738-743.
[18] K. Wu and M. D. Levine, 3D part segmentation: A new physics-based approach, *IEEE International symposium on Computer Vision*, 1995, pp. 311-316.
[19] N. Ahuja and J. H. Chuang, Shape Representation Using a Generalized Potential Field Model, *IEEE Transactions PAMI*, Vol. 19, No. 2, 1997, pp. 169-176.
[20] T. Grogorishin, G. Abdel-Hamid and Y.H. Yang, Skeletonization: An Electrostatic Field-Based Approach, *Pattern Analysis and Application*, Vol. 1, No. 3, 1996, pp. 163-177.
[21] Xiao-Dong Zhuang, Nikos E. Mastorakis, A magneto-statics inspired transform for structure representation and analysis of digital images, *WSEAS Transactions on Computers*, Vol. 8, No. 5, 2009, pp. 874-883.
[22] X. D. Zhuang, N. E. Mastorakis, A novel field-source reverse transform for image structure representation and analysis, *WSEAS Transactions on Computers*, Vol. 8, No. 2, 2009, pp. 376-385.
[23] P. Hammond, *Electromagnetism for Engineers: An Introductory Course*, Oxford University Press, USA, forth edition, 1997.
[24] I. S. Grant and W. R. Phillips, *Electromagnetism*, John Wiley & Sons, second edition, 1990.
[25] Terence W. Barrett, *Topological foundations of electromagnetism, World Scientific series in contemporary chemical physics*, Vol. 26, World Scientific, 2008.
[26] Minoru Fujimoto, *Physics of classical electromagnetism*, Springer, 2007.
[27] Gustavo Carneiro, Allan D. Jepson, Flexible Spatial Configuration of Local Image Features, *IEEE Transactions on Pattern Analysis and Machine Intelligence*, vol. 29, 2007, pp. 2089-2104.
[28] C. R. Shyu, C. E. Brodley, A. C. Kak, A. Kosaka, A. Aisen, L. Broderick, Local versus global features for content-based image retrieval, *IEEE Workshop on Content-Based Access of Image and Video Libraries*, 1998, pp. 30-34.
[29] Y. Shelepin, A. Harauzov, V. Chihman, S. Pronin, V. Fokin, N. Foreman, Incomplete image perception: Local features and global description, *International Journal of Psychophysiology*, Vol. 69, Issue 3, 2008, pp. 164.
[30] Aude Oliva, Antonio Torralba, Building the gist of a scene: the role of global image features in recognition, *Progress in brain research*, Vol. 155, 2006, pp. 23-36.
[31] Yuntao Qian, Rongchun Zhao, Image segmentation based on combination of the global and local information, *International Conference on Image Processing*, Vol. 1, 1997, pp. 204-207.
[32] J.A. Montoya-Zegarra, J. Beeck, N. Leite, R. Torres, A. Falcao, Combining Global with Local Texture Information for Image Retrieval Applications, *10th IEEE International Symposium on Multimedia*, 2008, pp. 148-153.
[33] M. Aly, P. Welinder, M. Munich, P. Perona, Automatic discovery of image families: Global vs. local features, *16th IEEE International Conference on Image Processing*, 2009, pp. 777-780.
[34] Dimitri A. Lisin, Marwan A. Mattar, Matthew B. Blaschko, Erik G. Learned-Miller, Mark C. Benfield, Combining Local and Global Image Features for Object Class Recognition, *Proceedings of the 2005 IEEE Computer Society Conference on Computer Vision and Pattern Recognition*, Vol. 03, 2005, pp. 47.
[35] Takahiro Toyoda, Osamu Hasegawa, Random Field Model for Integration of Local Information and Global Information, *IEEE Transactions on Pattern Analysis and Machine Intelligence*, Vol. 30, 2008, pp. 1483-1489
[36] Jiying Wu, Qiuqi Ruan, Gaoyun An, A novel image interpolation method based on both local and global information, *Proceedings of the intelligent computing 3rd international conference on advanced intelligent computing theories and applications*, 2007, pp. 842-851.